UBIQUITOUS MICROCHONDRULES IN THE MATRIX OF UNEQUILIBRATED ORDINARY CHONDRITES. E. Dobrică and A. J. Brearley, Department of Earth and Planetary Sciences, MSC03-2040, 1University of New Mexico, Albuquerque, NM 87131-0001, USA (edobrica@unm.edu).

Introduction: Chondrules are one of the most important components in all the chondrite groups (with the exception of the CI chondrites) and they are the most abundant component of ordinary chondrites (OCs, 60-80 vol%) [1]. These rounded to subrounded objects appear to have formed in the solar nebula by the rapid cooling of melt droplets; however, their exact formation mechanism remains enigmatic [1]. Although chondrules in all the chondrite groups typically have diameters >100 µm in size, studies of unequilibrated ordinary chondrites (UOCs) and different types of carbonaceous chondrites (CCs) have identified microchondrules (≤40 µm), embedded within the fine-grained matrix of these meteorites [2]. These microchondrules typically contain low-Ca pyroxene and FeO-bearing olivines [3-4].

In this study, a significant number of spherical objects similar in size to microchondrules were identified in the matrices of the two UOCs (MET 00526 - L3.05 and Semarkona - LL3.00 [5-6]); however, based on detailed Scanning Electron Microscopy (SEM), Transmission Electron Microscopy (TEM) and electron microprobe (EMPA) observations, about half of these new microchondrules are characterized by textures and chemical compositions that are distinct from those of previously described microchondrules [7]. We discuss the implications of these observations for the origin of the microchondrules and their connection to chondrules.

Methods: Thin sections of MET 00526 and Semarkona were initially studied on a FEI Quanta 3D FEGSEM/FIB operating at 30 kV using backscattered electron (BSE) imaging. After SEM characterization, quantitative bulk chemical compositions of the microchondrules were measured using a JEOL 8200 Superprobe electron microprobe (EMPA), operating at an acceleration voltage of 15 kV and a 20 nA beam current. TEM sections were prepared of 9 microchondrules (8 from MET 00526 and one from Semarkona) and one chondrule rim, using the focused ion beam (FIB) technique using the FEI Quanta 3D instrument. Bright and dark-field TEM images and quantitative EDS X-ray analyses were carried out at 200 kV on a JEOL 2010F FEG TEM/Scanning TEM (STEM).

Results: Microchondrules (µch.) represent about 800 ppm of MET 00526 (N = 710) and Semarkona (N = 647). They are characterized either by porous (48% - Semarkona and 43% - MET 00526) or smooth interiors (Fig. 1a, c). Their diameters vary between 1-50 µm with an average of ~6 µm for the microchondrules identified in MET 00526 and ~8 µm in Semarkona. More than half (≥60%) of the microchondrules occurs isolated in the matrix. We identified microchondrules with different morphologies, including spherical to subspherical and compound (two or more microchondrules joined together). The porous microchondrules contain pores distributed i) homogeneously throughout the entire microchondrule, ii) just within a zone around the edge of the microchondrule, iii) asymmetrically in the microchondrule and iv) only in the center of the microchondrule. The vesicles in each microchondrule can occupy up to 20% of the total surface area of the microchondrule as seen in the SEM and their sizes in each microchondrule vary between 0.3 and 3 µm. SEM observations show that several microchondrules contain euhedral crystalline phases.

In addition to the distinctive rounded to subrounded microchondrules, several irregularly-shaped objects and regions of chondrule rims with a similar porous texture have also been identified (Fig. 1e).

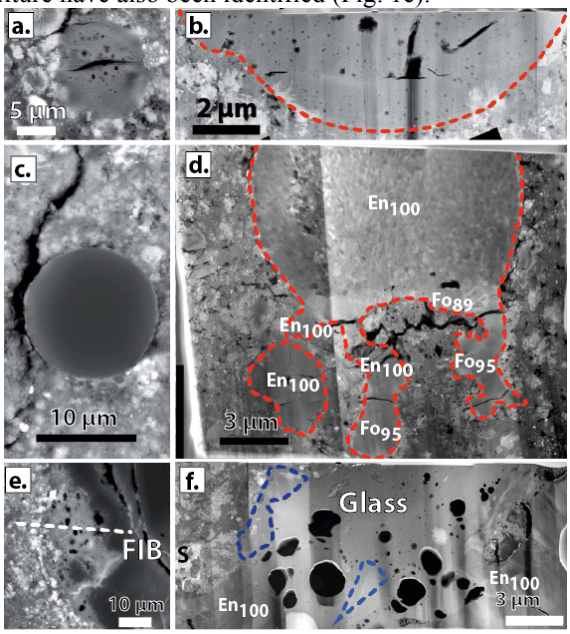

Figure 1. Backscattered electron SEM images of microchondrules (a – porous and c – smooth) and the outermost part of a chondrule (e) with a porous texture in MET 00526. Dark-field STEM images (b, d, f) of the FIB sections (white dashed line) analyzed. The red dashed lines show the sharp boundaries between the glassy, vesiculated microchondrules and the matrix. The blue dashed lines show the presence of Ca-rich pyroxenes ($En_{54}Wo_{46}$) in contact with the porous glass (Table 1) and low-Ca pyroxenes. Minor phases identified in the FIB sections: S = low-Ni sulfides, En = low-Ca pyroxene and Fo = forsterite.

The bulk chemical compositions of the porous and smooth microchondrules, the irregularly-shaped re-

gions and the outermost part of chondrule mesostasis with a porous vesicular texture were measured by EMPA in MET 00526 (Table 1). Several smooth microchondrules identified in this study have compositions close to the stoichiometry of olivines (Fo_{78-98}; N = 4) and pyroxenes (En_{85-99}; N = 14). The porous microchondrules in both meteorites are enriched in Na_2O, MgO and FeO compared with the smooth microchondrules (Table 1).

	Porous µch.		Smooth µch.		Ch. Rim Glass
	TEM	EMPA	TEM	EMPA	TEM
N	8	56	1	14	13
Na_2O	3.8	2.4	0	1.1	3.36
MgO	8.4	10.8	40.1	22.3	5.3
Al_2O_3	6.1	4.9	0	3.6	6.7
SiO_2	57.9	46.9	58.4	48.3	59.9
K_2O	0.5	0.5	0	0.3	0.3
CaO	1.6	1.9	0	1.4	1.3
TiO_2	0.1	0.1	0	0.1	0.0
Cr_2O_3	0.1	0.4	0.5	0.4	0.0
MnO	0.1	0.3	0.7	0.5	0.0
FeO	24.3	30.4	0.3	20.5	23.0
NiO	bd	0.5	bd	0.9	bd
SO_3	bd	0.7	bd	1.1	bd
P_2O_5	bd	0.1	bd	0.1	bd

Table 1. Concentrations of major and minor elements (in wt% oxide) determined by EDS (TEM) and WDS (EMPA) measurements in glassy vesiculated and smooth microchondrules (µch.) and the glassy rim of one chondrule from MET 00526 (N = number of µch; bd = below detection).

TEM studies show that microchondrules have sharp boundaries with the matrix; however, several regions present more diffuse boundaries due to partial aqueous alteration and formation of elongated ferroan olivine (Fa_{58}) crystals in the periphery of the microchondrule (Fig. 1, b) [e.g. 8]. The dominant constituent of the porous microchondrules (7 from MET 00526 and one from Semarkona) is glass with atomic Mg+Fe/Si ratios that vary between 0.4-1.0. The glass is FeO-rich (18.0-33.9 wt%) and contains significant amounts of other elements such as Na_2O (1.0-7.4 wt%) and Al_2O_3 (2.6-8.3 wt%). No evidence of chemical zoning was observed in the microchondrules analyzed. TEM observations show that the vesicles have irregular morphologies and sizes (a few nm to 1 µm) that are not related to the size of the object. Only one smooth microchondrule from MET 00526 has been analyzed so far and it is composed of crystals (avg. 500 nm, up to 1.4 x 0.6 µm) of enstatite (En_{98-100}). The lower part of this microchondrule contains several olivine (Fo_{89}) crystals (Fig. 1d). These crystals are in direct contact with irregularly-shaped olivines with a similar chemical composition (Fo_{89-95}) and pyroxenes (En_{100}) which suggest a continuation of the microchondrule and a loss of the rounded morphology in this region.

One additional FIB section was prepared from a region at the edge of a type I porphyritic olivine-pyroxene chondrule. This region exhibited the same vesicular texture as the porous microchondrules (Fig. 1e, f). TEM observations show that this material is a vesiculated glass with a similar composition to the porous microchondrules (Table 1). Ca-rich pyroxenes enriched in MnO and Cr_2O_3 (up to 1.4 wt% MnO and 2.5 wt% Cr_2O_3, respectively) and low-Ca pyroxenes were identified in contact with the glass.

Discussion: The fine-grained matrices of two UOCs contain ubiquitous, randomly distributed microchondrules. Their abundance (~0.08 vol% for µch. ≤40 µm) is up to 160 times higher than the values proposed by previous studies [4]. Their spherical morphology and the presence of a glassy material indicate that they were once molten free-floating droplets. The glass in the porous microchondrules contains high Na contents indicating that the precursors of these objects were volatile-rich. The vesicles may have formed by loss of Na or other volatile elements during melting. These glassy microchondrules suggest that degassing occurred during the melting episode of microchondrule formation. The fact that such small objects only underwent partial degassing and were quenched to a glass indicates exceptionally fast heating and cooling rates.

The bulk composition of porous microchondrules is distinct from the average composition of mesostasis in chondrules measured in the same meteorite [5]. Although, the range of SiO_2 (49.7-58.1 wt%) and Na_2O 2.1-6.6 wt%) contents of porous microchondrules overlap the range of mesostasis compositions (44.1-76.3 wt% SiO_2; 0.1-10.8 wt% Na_2O) measured in 20 chondrules from MET 00526 [9], the ranges of Al_2O_3 and FeO are distinct. Al_2O_3 contents in porous microchondrules (4.1-7.8 wt%) are lower than those found in chondrule mesostasis (8.3-32.7 wt%) and FeO is significantly higher in microchondrules (µch. – 18.2-31.9 wt% FeO vs 0.4-16.7 wt% FeO in chondrule mesostasis). The FeO content of microchondrules is however, similar to that of the bulk matrix composition.

Our preliminary observations show that the porous microchondrules seem to have formed in the same region as chondrules. They appear to have collided with chondrules while they were still in a molten state, prior to accretion.

Acknowledgements: This work was funded by NASA Cosmochemistry grant NNG06GG37G and NNX11AK51G to A. J. Brearley (PI).

References: [1] Jones, R. H., et al. (2000). *Protostars and Planets IV*: 927. [2] Krot, A. N., et al., (2003). *Treatise on Geochemistry*, Vol. 1., Elsevier-Pergamon. [3] Krot, A. N., et al. (1997). *Geochim. Cosmochim. Acta* **61**: 463-473. [4] Rubin, A. E., et al. (1982). *Geochim. Cosmochim. Acta* **46**: 1763-1776. [5] Grossman J.N. and Brearley A.J. (2005) *Meteorit. Planet. Sci.* **40**, 87. [6] Berlin J.*, et al.* (2011) *Meteorit. Planet. Sci.* **46**(4), 513-533. [7] Dobrică, E. and A. J. Brearley (2012). LPSC **43:** 2197. [8] Dobrică, E. and A. J. Brearley (2012). LPSC **43:** 2212. [9] Berlin J. (2009) Ph.D. thesis, University of New Mexico, Albuquerque, NM.